

Published in final edited form as:

Neuron. 2011 July 14; 71(1): 92–102. doi:10.1016/j.neuron.2011.04.021.

A neuropeptide-mediated stretch response links muscle contraction to changes in neurotransmitter release

Zhitao Hu^{1,2}, Edward C.G. Pym^{1,2}, Kavita Babu^{1,2}, Amy B. Vashlishan Murray^{1,2}, and Joshua M. Kaplan^{1,3}

¹ Department of Molecular Biology, Massachusetts General Hospital, Boston, MA 02114; Department of Neurobiology, Harvard Medical School, Boston, MA 02115

² Department of Communication Sciences & Disorders, Emerson College, Boston, MA 02116

Abstract

Although *C. elegans* has been utilized extensively to study synapse formation and function, relatively little is known about synaptic plasticity in *C. elegans*. We show that a brief treatment with the cholinesterase inhibitor aldicarb induces a form of presynaptic potentiation whereby ACh release at neuromuscular junctions (NMJs) is doubled. Aldicarb-induced potentiation was eliminated by mutations that block processing of pro-neuropeptides, by mutations inactivating a single pro-neuropeptide (NLP-12), and by those inactivating an NLP-12 receptor (CKR-2). NLP-12 expression is limited to a single stretch-activated neuron, DVA. Analysis of a YFP-tagged NLP-12 suggests that aldicarb stimulates DVA secretion of NLP-12. Mutations disrupting the DVA mechanoreceptor (TRP-4) decreased aldicarb-induced NLP-12 secretion and blocked aldicarb-induced synaptic potentiation. Mutants lacking NLP-12 or CKR-2 have decreased locomotion rates. Collectively, these results suggest that NLP-12 mediates a mechanosensory feedback loop that couples muscle contraction to changes in presynaptic release, thereby providing a mechanism for proprioceptive control of locomotion.

Keywords

C. elegans; neuromuscular junction; synaptic plasticity; dense core vesicle; neuropeptide; TRP channel; TRP-4; NLP-12; proprioceptor

Introduction

Neuropeptides represent a vast and chemically diverse set of neurotransmitters. Pro-neuropeptides are packaged into large dense core vesicle (DCV) precursors, where they are processed into active forms by co-packaged enzymes. Many, and perhaps all, neurons express and secrete neuropeptides. Expression of specific neuropeptides is often utilized as a marker to distinguish subclasses of neurons. For example, subclasses of mouse cortical

© 2011 Elsevier Inc. All rights reserved.

³Corresponding author: Joshua M. Kaplan, Ph.D., Department of Molecular Biology, Massachusetts General Hospital, Richard B Simches Research Building, 185 Cambridge Street CPZN 7250, Boston, MA 02114-2790, Tel: 617-726-5900, Fax: 617-726-5949, kaplan@molbio.mgh.harvard.edu.

²These authors contributed equally.

Publisher's Disclaimer: This is a PDF file of an unedited manuscript that has been accepted for publication. As a service to our customers we are providing this early version of the manuscript. The manuscript will undergo copyediting, typesetting, and review of the resulting proof before it is published in its final citable form. Please note that during the production process errors may be discovered which could affect the content, and all legal disclaimers that apply to the journal pertain.

interneurons are distinguished by their expression of cholecystokinin and somatostatin (Kawaguchi and Kondo, 2002). Despite their widespread expression, relatively little is known about how specific neuropeptides function within circuits.

Secretion of neuromodulatory peptides has often been proposed as a mechanism for regulating synaptic efficacy and producing adaptive changes in behavior; however, genetic studies of neuropeptide function have primarily focused on endocrine functions. In a few cases, the impact of specific neuropeptides has been explored in particular circuits. For example, specific neuropeptides have been implicated in adaptation of odorant responses (Chalasanani et al., 2010; Ignell et al., 2009), in ethanol sensitivity (Davies et al., 2004; Moore et al., 1998), and in regulation of circadian behaviors (Lear et al., 2005; Mertens et al., 2005; Renn et al., 1999). Much remains to be learned about how neuropeptides shape the function of these and other behavioral circuits.

The nematode *C. elegans* has been utilized as a genetic model to study neuropeptide function. The genome sequence predicts 115 proneuropeptide genes, encoding 250 different mature peptides (Li and Kim, 2008). Many of these predicted peptides have been confirmed by mass spectrometry (Husson et al., 2006; Husson et al., 2007; Husson and Schoofs, 2007). Mutations have been described that disrupt proneuropeptide processing (*egl-3* PC2, *egl-21* CPE, and *sbt-1* 7B2), maturation of DCVs (*unc-108* Rab2 and *ric-19* ICA69), and exocytosis of DCVs (*unc-31* CAPS and *pkc-1* PKC ϵ) (Edwards et al., 2009; Husson and Schoofs, 2007; Jacob and Kaplan, 2003; Kass et al., 2001; Sieburth et al., 2005; Sieburth et al., 2007; Speese et al., 2007; Sumakovic et al., 2009). Hereafter, we refer to these mutants collectively as neuropeptide-deficient mutants.

Several prior studies suggested that neuropeptides regulate transmission at cholinergic NMJs in *C. elegans*. Sensitivity of *C. elegans* to paralysis induced by the cholinesterase inhibitor aldicarb has been used as a measure of acetylcholine release (ACh) at neuromuscular junctions (Miller et al., 1996). Mutations that decrease ACh secretion confer resistance to aldicarb-induced paralysis (Nonet et al., 1998; Saifee et al., 1998) while those that increase ACh secretion cause aldicarb hypersensitivity (Gracheva et al., 2006; McEwen et al., 2006; Vashlishan et al., 2008). Many neuropeptide deficient mutants are aldicarb resistant, implying that endogenous neuropeptides regulate synaptic transmission (Edwards et al., 2009; Husson and Schoofs, 2007; Jacob and Kaplan, 2003; Kass et al., 2001; Sieburth et al., 2005; Sieburth et al., 2007; Speese et al., 2007; Sumakovic et al., 2009); however, the synaptic basis for the aldicarb resistance of neuropeptide mutants has not been determined. Electrophysiological recordings have been reported for four neuropeptide deficient mutants. In three cases (*pkc-1* PKC ϵ , *unc-108* Rab2, and *ric-19* ICA69 mutants), baseline transmission was unaltered whereas in the fourth case (*unc-31* CAPS) transmission was modestly reduced (Edwards et al., 2009; Gracheva et al., 2007; Sieburth et al., 2007; Sumakovic et al., 2009). This discrepancy may reflect the fact that CAPS has also been proposed to directly promote SV exocytosis (Jockusch et al., 2007). Thus, it remains unclear how neuropeptides alter neuromuscular signaling.

Here we show that aldicarb treatment potentiates ACh release in wild type animals, that the neuropeptide NLP-12 is required for this effect, and that NLP-12 is secreted by a stretch-activated mechanosensory neuron (DVA). Collectively, our results suggest that NLP-12 provides proprioceptive feedback that couples muscle contraction to changes in presynaptic release. These results provide a synaptic mechanism for proprioceptive control of locomotion behavior.

Results

Mutants lacking *egl-3* PC2 have wild type baseline synaptic transmission

To further address the impact of endogenous neuropeptides on cholinergic transmission, we recorded excitatory post-synaptic currents (EPSCs) from adult body muscles of *egl-3* PC2 mutants (Fig. 1). The *egl-3* gene encodes a protease that is most similar to proprotein convertase type 2 (PC2) (Kass et al., 2001) and *egl-3* PC2 mutants have severe defects in proneuropeptide processing (Husson et al., 2006; Jacob and Kaplan, 2003). Like other neuropeptide deficient mutants, *egl-3* mutants were resistant to aldicarb-induced paralysis (Fig. 1I) (Jacob and Kaplan, 2003). We recorded both endogenous EPSCs, which are synaptic events mediated by the endogenous activity of cholinergic motor neurons, as well as EPSCs evoked by a depolarizing stimulus. In *egl-3* null mutants, the rate, amplitude, and kinetics of endogenous EPSCs, and the amplitude and total synaptic charge of evoked EPSCs were all unaltered compared to wild type controls (Figs. 1 and S1, Table S1). These results are consistent with prior studies of several other neuropeptide defective mutants (e.g. *pkc-1* PKC ϵ , *unc-108* Rab2, and *ric-19* ICA69) (Edwards et al., 2009; Sieburth et al., 2007; Sumakovic et al., 2009). Aldicarb resistance can also arise from increased transmission at GABAergic NMJs (Mullen et al., 2006), which could potentially explain the phenotype of neuropeptide mutants. To test this possibility, we recorded inhibitory post-synaptic currents (IPSCs) from adult body muscles. The rate and amplitude of endogenous IPSCs observed in *egl-3* PC2 mutants were indistinguishable from those observed in wild type controls (Fig. S1A–C). Collectively, these results suggest that changes in baseline transmission at cholinergic or GABAergic NMJs cannot account for the aldicarb resistance of neuropeptide mutants.

Aldicarb treatment potentiates cholinergic transmission

Aldicarb sensitivity is assayed by measuring the onset of paralysis during a two hour aldicarb treatment. Given the prolonged time course of these assays, we reasoned that aldicarb exposure might alter synaptic transmission, which could account for the discrepancy between the behavioral and electrophysiological phenotypes of the neuropeptide mutants. To test this idea, we recorded body muscle EPSCs after a 60 minute pre-treatment with aldicarb. Aldicarb treatment significantly increased the rate of endogenous EPSCs, and the total synaptic charge of evoked EPSCs, both indicating enhanced cholinergic transmission (Fig. 1A–F, and Table S1). By contrast, aldicarb treatment did not alter the IPSC rate of either wild type or *egl-3* mutants, suggesting that this effect was specific for cholinergic transmission (Fig. S1A–B).

The synaptic potentiation following aldicarb treatment could be caused by either a pre- or post-synaptic change. The increased rate of endogenous EPSCs suggests a pre-synaptic origin for the potentiation. Nonetheless, we did several additional experiments to rule out post-synaptic changes. First, aldicarb treatment did not alter the amplitude or kinetics of endogenous EPSCs (Figs. 1C, S1D–F, and Table S1), both suggesting that muscle sensitivity to synaptically released ACh was unaltered. Second, aldicarb treatment did not increase the amplitude of currents activated by application of exogenous ACh (Fig. 1G–H, and Table S1). In fact, ACh activated currents were significantly decreased by aldicarb treatment. Third, aldicarb treatment did not increase the abundance of GFP-tagged ACR-16 nicotinic receptors in body muscles (K Babu, manuscript in preparation). Therefore, aldicarb induced synaptic potentiation was more likely caused by a presynaptic change in ACh release.

NLP-12 is required for aldicarb-induced synaptic potentiation

The resistance of neuropeptide deficient mutants to aldicarb-induced paralysis could be caused by defects in aldicarb-induced synaptic potentiation. Consistent with this idea, the aldicarb-induced increase in EPSC rate and in evoked synaptic charge were both eliminated in *egl-3* PC2 mutants (Fig. 1B and F, Table S1). This lack of aldicarb-induced potentiation was not caused by a generalized defect in synaptic transmission because endogenous and evoked EPSCs observed in untreated *egl-3* PC2 mutants were indistinguishable from wild type controls (Fig. 1 and S1, and Table S1).

In a large RNAi screen, we found that inactivation of several proneuropeptide encoding genes (including *ins-22*, *ins-31*, *flp-1*, and *nlp-12*) causes resistance to aldicarb-induced paralysis (Sieburth et al., 2005). Aldicarb resistance phenotypes were confirmed for *flp-1* and *nlp-12* using available knockout alleles (Sieburth et al., 2005). The aldicarb resistance of *nlp-12* mutants was much stronger than that of *flp-1* mutants; consequently, we focused our subsequent analysis on *nlp-12*.

If an *nlp-12* encoded neuropeptide mediates aldicarb-induced paralysis and synaptic potentiation, then *nlp-12* and *egl-3* mutations should have very similar effects on behavior and synaptic transmission. Several results support this idea. First, *nlp-12* and *egl-3* mutations did not have additive effects on aldicarb-induced paralysis, consistent with their functioning together in this process (Fig. 2C). Second, baseline endogenous and evoked EPSCs were unaltered in *nlp-12* single mutants (Figs. 2, S2, and Table S2), as was the case in *egl-3* PC2 mutants (Figs. 1, S1, and Table S1). Third, the aldicarb-induced increases in EPSC rate and evoked synaptic charge were both eliminated in *nlp-12* mutants, and were restored by a transgene containing an *nlp-12* genomic clone (Fig. 2). Collectively, these results support the idea that an *nlp-12* encoded peptide is required for the behavioral and synaptic effects of aldicarb.

An NLP-12 receptor, CKR-2, is also required for aldicarb-induced potentiation

The *ckr-2* gene encodes a G-protein coupled receptor that is most similar to mammalian gastrin receptors (Janssen et al., 2008). NLP-12 peptides are high affinity agonists for CKR-2 receptors expressed in tissue culture cells (Janssen et al., 2008). Prompted by these results, we tested *ckr-2* mutants for defects in aldicarb-induced paralysis and synaptic potentiation. Like *nlp-12* mutants, *ckr-2* mutants were resistant to aldicarb-induced paralysis, had normal baseline cholinergic transmission, but lacked aldicarb-induced increases in EPSC rate and evoked synaptic charge (Figs. 3 and S3, Table S3). The *nlp-12* and *ckr-2* mutations did not have additive effects on aldicarb-induced paralysis nor on baseline synaptic transmission (Fig. 3C, Table S3). A transcriptional reporter containing the *ckr-2* promoter was expressed in both cholinergic and GABAergic motor neurons (Fig. 3F). The behavioral and electrophysiological defects of *ckr-2* mutants were rescued by transgenes expressing CKR-2 in all cholinergic neurons (using the *unc-17* VACHT promoter), in cholinergic motor neurons (using the *acr-2* promoter), but not by those expressed in GABAergic neurons (using the *unc-25* GAD promoter) (Fig. 3 and Table S3). These results suggest that CKR-2 functions in cholinergic neurons, mediating the effects of aldicarb on behavior and synaptic transmission.

Thus far, our results are most consistent with the idea that NLP-12's effects on cholinergic transmission are pre-synaptic. By contrast, a prior study showed that NLP-12 application induces contraction of isolated *A. suum* muscle strips (McVeigh et al., 2006), suggesting a direct effect on muscle. Based on these results, we did several additional experiments to determine if NLP-12 and CKR-2 have post-synaptic effects. First, we analyzed ACh-activated muscle currents, finding that the currents recorded from untreated *nlp-12* and *ckr-2*

mutants were indistinguishable from wild type controls (Figs. S2D–E and S3D–E, Tables S2 and S3). Second, aldicarb treatment significantly reduced the amplitude of ACh activated currents in wild type muscles (Fig. 1G–H, Table S1), and identical effects were observed in aldicarb-treated *nlp-12* (Fig. S2D–E, Table S2) and *ckr-2* (Fig. S3D–E, Table S3) mutant muscles. Third, to assess muscle responses to synaptically released ACh, we analyzed endogenous EPSCs. We found that neither the amplitude nor the kinetics of endogenous EPSCs were significantly altered in control and aldicarb treated wild type (Fig. S1D–F, Table S1), *nlp-12* (Fig. S2A–C, Table S2), and *ckr-2* (Fig. S3A–C, Table S3) animals. Thus, changes in muscle responsiveness to ACh were not observed in *nlp-12* and *ckr-2* mutants. Finally, the *ckr-2* transcriptional reporter was not expressed in body muscles (data not shown). Collectively, our results are most consistent with the idea that NLP-12 and CKR-2 potentiate cholinergic transmission through a presynaptic mechanism.

NLP-12 is expressed in DVA neurons

We analyzed a reporter construct containing the *nlp-12* promoter driving expression of GFP. This reporter construct was expressed in a single tail neuron, DVA, consistent with prior studies (Janssen et al., 2008).

Fluorescently-tagged proneuropeptides have been used to monitor secretion in *C. elegans* (Ch'ng et al., 2008; Sieburth et al., 2007); therefore, we reasoned that a similar approach could be utilized to analyze NLP-12 secretion. Expression of NLP-12::YFP in DVA (using the *nlp-12* promoter) showed a punctate distribution in the DVA axon, in both the ventral nerve cord and in the nerve ring (Fig. 4A). Several results suggest that the NLP-12 puncta correspond to DCVs containing NLP-12::YFP. First, expression of the NLP-12::YFP transgene rescued the *nlp-12* mutant defects in aldicarb-induced paralysis (Fig. 2C) and synaptic potentiation (data not shown), demonstrating that the tagged proneuropeptide retains biological activity. Second, NLP-12 puncta fluorescence was significantly increased in *unc-13* Munc13 mutants (which are defective for DCV secretion) (Sieburth et al., 2007; Speese et al., 2007) (Figs. 4A–B and S4C–D). Taken together, these results indicate that DVA neurons express and actively secrete NLP-12.

NLP-12::YFP behaved differently from other neuropeptide constructs that we previously analyzed. For other neuropeptides (e.g. NLP-21::YFP expressed in DA motor neurons), YFP secreted by neurons is taken up by specialized phagocytic cells in the body cavity (termed coelomocytes), where it can be quantified as a fluorescent signal (Sieburth et al., 2007). For NLP-12::YFP, we were unable to detect coelomocyte fluorescence (Fig. S4F). This distinction apparently results from expression of NLP-12 in the DVA neuron, which has an axon in the ventral nerve cord. When NLP-12::YFP was expressed in DA neurons, we observed fluorescent puncta in both dorsal cord axons and in coelomocytes (Fig. S4E); however, this transgene was unable to rescue the *nlp-12* mutant defect in aldicarb-induced paralysis (Fig. 2C). Conversely, when NLP-21::YFP was expressed in DVA, coelomocyte fluorescence was not detected (data not shown). These results suggest that YFP secreted in the ventral nerve cord cannot be internalized by coelomocytes, perhaps because it is endocytosed by another cell type (e.g. the ventral hypodermis, or body muscles) or cannot efficiently diffuse out of the ventral cord tissue.

Aldicarb treatment stimulates NLP-12 secretion from DVA neurons

If NLP-12 mediates the effects of aldicarb on behavior and synaptic transmission, we would expect that aldicarb treatment would stimulate NLP-12 secretion from DVA. Consistent with this idea, we found that aldicarb treatment resulted in a rapid and significant decrease in NLP-12 puncta fluorescence in DVA axons (Figs. 4A–B and S4A). This effect was specific for NLP-12 secretion by DVA, as aldicarb treatment did not decrease NLP-21

puncta fluorescence in DA motor neurons (Fig. 4C–D). The effect of aldicarb on NLP-12 puncta fluorescence was eliminated in both *unc-31* CAPS and *unc-13* Munc13 mutants (Figs. 4B and S4C–D), implying that the aldicarb induced decrease in NLP-12 puncta fluorescence was mediated by increased NLP-12 secretion. These results support the idea that aldicarb stimulates NLP-12 secretion by DVA neurons, thereby potentiating cholinergic transmission and paralysis. Consistent with this idea, a transgene driving NLP-12 expression in DA motor neurons failed to rescue the *nlp-12* mutant aldicarb induced paralysis defect (Fig. 2C), suggesting that expression in DVA is critical for NLP-12's function.

TRP-4 is required for aldicarb-induced plasticity

DVA has been previously proposed to function as a stretch receptor (Li et al., 2006). Bending of the worm's body induces calcium transients in DVA, that are eliminated in mutants lacking TRP-4, a mechanically-gated ion channel (Kang et al., 2010; Li et al., 2006). Prompted by these results, we tested the idea that aldicarb-induced muscle contraction provides a mechanical stimulus that induces NLP-12 secretion. Consistent with this idea, the aldicarb-induced decrease in NLP-12 puncta fluorescence was significantly reduced in *trp-4* mutants (Figs. 4A–B and S4B). This suggests that the ability of DVA to sense mechanical stimuli is required to stimulate NLP-12 secretion.

If TRP-4 is required for aldicarb-induced NLP-12 secretion, then we would expect that *trp-4* mutants would have behavioral and electrophysiological defects similar to those observed in *nlp-12* mutants. As expected, *trp-4* mutants were resistant to aldicarb-induced paralysis (Fig. 5F). In addition, like *nlp-12* mutants, *trp-4* mutants lacked the aldicarb-induced increase in EPSC rate (Fig 5A–B) and in evoked synaptic charge (Fig 5D–E), while baseline cholinergic transmission was unaltered. Collectively, these results suggest that aldicarb-induced body muscle contractions induce NLP-12 secretion, which subsequently potentiates ACh secretion pre-synaptically.

NLP-12 regulates locomotion behavior

Thus far, our results suggest that NLP-12 mediates a mechanosensory feedback loop that couples muscle contraction (induced by aldicarb treatment) to changes in pre-synaptic ACh release. To determine if NLP-12 signaling has an impact in the absence of aldicarb, we analyzed the locomotion behavior of *nlp-12* mutants. A prior study showed that bending of the worm's body during swimming behavior induces calcium transients in DVA (Li et al., 2006); consequently, we would expect that NLP-12 secretion from DVA would also occur during normal locomotion behavior. To assess changes in locomotion, we measured the velocity of worm locomotion. We found that locomotion rate was significantly reduced in *nlp-12* mutants and that this defect was rescued by an *nlp-12* transgene (Fig. 6A–B). A similar locomotion defect was also observed in *ckr-2* mutants, which was rescued by a *ckr-2* transgene expressed in cholinergic motor neurons (using the *acr-2* promoter) (Fig. 6A–B). These results suggest that NLP-12 secretion modulates locomotion, consistent with the idea that this mechanosensory feedback mechanism is engaged during locomotion behavior.

To further investigate the connection between NLP-12 secretion and locomotion rate, we analyzed NLP-12 secretion in strains that have differing locomotion rates (Fig. 6C). This analysis shows that increased locomotion rates (in *npr-1* mutants) are correlated with decreased NLP-12 puncta fluorescence, whereas slow locomotion (in *mec-3* mutants) was accompanied by increased NLP-12 puncta fluorescence. Thus, changes in locomotion rate are accompanied by corresponding changes in NLP-12 secretion.

Discussion

We describe a mechanosensory feedback mechanism whereby muscle contraction is coupled to changes in ACh release at NMJs. This feedback mechanism consists of a stretch sensitive neuron (DVA), which secretes the neuropeptide NLP-12 in response to muscle contraction. Activation of CKR-2, an NLP-12 receptor, potentiates transmission at cholinergic NMJs. This mechanosensory feedback is employed during spontaneous locomotion behavior to determine locomotion rate. These experiments define the synaptic basis for a simple proprioceptive feedback circuit.

Activity-dependent plasticity at *C. elegans* synapses

Aldicarb induced paralysis has been extensively utilized as a screening tool to identify *C. elegans* genes required for synaptic transmission. Many genes identified as aldicarb resistant mutants were subsequently shown to encode essential components of the presynaptic release machinery (Sieburth et al., 2005). Thus, it was somewhat surprising that neuropeptide deficient mutants, which are all strongly aldicarb resistant, have unaltered baseline synaptic physiology. Our results provide an explanation for this puzzle. We show that brief aldicarb treatments induce a form of synaptic potentiation, which is abolished in the neuropeptide deficient mutants. Several aspects of these results are significant. These results represent the first *C. elegans* paradigm for activity induced synaptic potentiation, and the first study to document an electrophysiological effect of an endogenous *C. elegans* neuropeptide. Our results also suggest that additional genes involved in synaptic plasticity will be found among the genes identified in the prior screens for aldicarb resistant mutants.

NLP-12 potentiates ACh release at NMJs

Here we show that secretion of NLP-12 potentiates synaptic transmission at cholinergic NMJs, and that it does so by enhancing ACh release. Aldicarb treatment enhanced cholinergic transmission, which was manifest by both an increase in the rate of EPSCs, and as an increase in the total synaptic charge evoked by a depolarizing stimulus. Both effects of aldicarb were eliminated by mutations inactivating NLP-12 and CKR-2 (an NLP-12 receptor). NLP-12 is expressed by a single neuron DVA, and aldicarb treatment induces NLP-12 secretion from these neurons. Collectively, these results support the idea that aldicarb treatment evokes NLP-12 secretion from DVA neurons, which subsequently potentiates cholinergic transmission.

Several results suggest that the NLP-12 mediated potentiation occurs by a presynaptic mechanism. First, the increase in endogenous EPSCs frequency is characteristic of a presynaptic change. Second, the amplitude and kinetics of endogenous EPSCs were not altered by aldicarb treatment, implying that muscle responses to individual synaptic quanta were unaltered. Third, ACh-activated muscle currents were not increased by aldicarb, suggesting that increased muscle sensitivity to ACh is unlikely to explain the aldicarb induced synaptic potentiation. In fact, aldicarb treatment significantly decreased ACh-activated current amplitudes, consistent with decreased muscle sensitivity to ACh. Identical decreases in ACh-activated currents were observed in aldicarb treated *nlp-12* and *ckr-2* mutants, suggesting that this effect was not mediated by NLP-12. Fourth, the *ckr-2* mutant defects in aldicarb-induced potentiation, aldicarb-induced paralysis, and locomotion rate were all rescued by transgenes expressing CKR-2 in the presynaptic cholinergic neurons. Fifth, a *ckr-2* transcriptional reporter was expressed in cholinergic motor neurons, but was not expressed in body muscles. Collectively, these results all support the idea that increased ACh release accounts for NLP-12 mediated potentiation of synaptic transmission.

Role of DVA as a mechanosensory neuron

A prior study showed that DVA neurons are stretch sensitive (Li et al., 2006). Stretch sensitivity of DVA was documented by observing calcium transients in DVA that are phasically activated by body bends during swimming behavior (Li et al., 2006). These swimming-induced DVA calcium transients were eliminated in mutants lacking TRP-4, a mechanoreceptor (Kang et al., 2010; Li et al., 2006).

Our results suggest that muscle contraction provides a mechanical stimulus that induces DVA secretion of NLP-12. NLP-12 is expressed only in DVA neurons, and it has a punctate distribution in DVA axons, consistent with its packaging into dense core vesicles (DCVs). Aldicarb treatment induces body muscle contraction, which is accompanied by decreased NLP-12 fluorescence in DVA axons. This aldicarb-induced decrease of NLP-12 fluorescence is blocked by *unc-31* CAPS and *unc-13* Munc13 mutations (which prevent DCV exocytosis), and is diminished by *trp-4* mutations (which eliminate the mechanosensitivity of DVA). By contrast, aldicarb had little effect on secretion of neuropeptides expressed by the DA motor neurons, implying that the effects of aldicarb on secretion are specific to neuropeptides expressed by the DVA neurons. Collectively, these results strongly support the idea that muscle contraction provides a mechanical stimulus that evokes increased NLP-12 secretion from DVA. Electron microscopic analysis of the ventral nerve cord also supports this idea. In the serial section reconstruction of the nervous system, the DVA axon typically lies in a dorsal position in the ventral nerve cord, adjacent to both a muscle cell membrane, and to axons of cholinergic motor neurons (typically VB neurons) (Fig. S5) (White et al., 1986) (www.wormimage.org). Thus, the DVA axon is well positioned for its function as a sensor of body muscle contraction, and for transducing this signal into altered cholinergic transmission.

Mechanosensory control of locomotion

In addition to its mechanosensory properties, DVA neurons were proposed to regulate specific aspects of worm locomotion, including the extent and speed of body bends during locomotion (Li et al., 2006). Based on these observations, it was proposed that DVA neurons act as stretch receptors, and perhaps function in a manner analogous to proprioceptive neurons. However, the synaptic basis for DVA mediated regulation of locomotion had not been described.

Our results provide a potential mechanism for DVA mediated regulation of locomotion rate. In particular, we propose that body bends occurring during locomotion promote NLP-12 secretion from DVA neurons, thereby enhancing ACh release at NMJs. Consistent with this idea, the locomotion rate of *nlp-12* and *ckr-2* mutants was significantly reduced compare to wild type controls. This locomotion defect provides support for the idea that NLP-12 secretion occurs during normal locomotion behavior, and that NLP-12 signaling is employed to modulate the pattern of locomotion. We propose that NLP-12 is utilized as an internal measure of recent locomotory activity. In particular, during periods of elevated locomotion rates (e.g. during local search for food), increased body movements lead to a net increase in NLP-12 secretion which would promote the continued high rate of locomotion through enhanced ACh release. A similar model was previously proposed for DVA function, based on the locomotion defects caused by laser killing DVA neurons (Wicks and Rankin, 1995). In these experiments, killing DVA neurons resulted in decreased forward and reverse locomotion responses to a mechanical stimulus. Based on these results, these authors proposed that DVA provides a gain control that amplifies the locomotory response of animals to mechanical stimuli (Wicks et al., 1996). Our results provide a potential synaptic mechanism for these behavioral effects.

Methods

Strains

Strain maintenance and genetic manipulation were performed as described (Brenner, 1974). Animals were cultivated at 20°C on agar nematode growth media seeded with OP50 bacteria.

KP5994 *nlp-12(ok335)I*
 LSC32 *ckr-2(tm3082)III*
 TQ296 *trp-4(sy695)I*
 CB1338 *mec-3(e1338)IV*
 KP6048 *npr-1(ky13)X*
 KP6199 *nlp-12(ok335)I; ckr-2(tm3082)III*
 KP6405 *nuIs441 (Pnlp-12::nlp-12::YFP)*
 KP6377 *unc-13(s69)I; nuIs441*
 KP6373 *unc-31(e928)IV; nuIs441*
 KP6376 *trp-4(sy695)I; nuIs441*
 KP6406 *trp-4(sy695)I; nuIs441* 1x out-crossed
 KP6545 *mec-3(e1338)IV; nuIs441*
 KP6546 *npr-1(ky13)X; nuIs441*
 BC168 *unc-13(s69)I*
 CB928 *unc-31(e928)IV*
 KP3945 *nuIs181 (Punc-129::nlp-21::YFP)*
 KP5966 *egl-3(nr2090)V*
 KP6202 *nlp-12(ok335)I; egl-3(nr2090)V*

Extrachromosomal arrays

KP6450 *nuEx1476 (Punc-25::ckr-2)*
 KP6449 *nuEx1475 (Punc-17::ckr-2)*
 KP6575 *nuEx1500 (Pacr-2::ckr-2::YFP)*
 KP6319 *nuEx1463 (Pnlp-12::nlp-12::YFP)*
 KP6404 *nuEx1474 (Pnlp-12::nlp-21::YFP)*
 KP6551 *nuEx1487 (Punc-129::nlp-12::YFP)*
 KP6552 *nuEx1488 (Punc-129::nlp-12::YFP)*
 KP6577 *nuIs392, nuEx1501 (Punc-17::mCherry + Pckr-2::NLS::GFP)*
 KP6578 *nuIs428, nuEx1501 (Punc-25::mCherry + Pckr-2::NLS::GFP)*

Constructs and transgenes

Pnlp-12::nlp-12::YFP—A 2.1kb *nlp-12* genomic region, 383bp upstream of the start codon and 1374bp downstream of the stop codon, was amplified by PCR. The stop codon of

nlp-12 was replaced by an MluI site by overlap extension PCR, and YFP (venus) was inserted in the MluI site, and its orientation confirmed by sequencing.

Punc-129::*nlp-12*::YFP—A cDNA corresponding to *nlp-12* was amplified by PCR and inserted into KP#1284 using gateway cloning (Sieburth et al., 2005).

***ckr-2* rescue**—A CKR-2a cDNA clone (Jannssen et al, 2008) was kindly provided by Liliane Schoofs. The cDNA was ligated into expression vectors (pPD49.26) containing the *unc-17* promoter (for cholinergic rescue), the *acr-2* promoter (for cholinergic motor neuron rescue), or the *unc-25* promoter (for GABAergic rescue).

***ckr-2* transcriptional reporter**—An 8.5 kb fragment of *ckr-2* genomic region, from 3008bp upstream of the start codon to 20bp into the second exon, was fused to a GFP containing 4 nuclear localization signals.

Transgenes and Germline Transformation

Transgenic strains were isolated by microinjection of various plasmids using either *Pmyo-2*::NLS-GFP (KP#1106) or *Pmyo-2*::NLS-mCherry (KP#1480) as co-injection markers. Integrated transgenes were obtained by UV irradiation of strains carrying extrachromosomal arrays. All integrated transgenes were out-crossed at least 6 times.

Locomotion and behavior assays

For aldicarb paralysis, between 18–25 young adult worms were transferred to plates containing 1.5mM aldicarb and assayed for paralysis as described previously (Nurrish et al., 1999). Worm tracking and analysis were performed similar to previous studies (Dittman and Kaplan, 2008) with minor modifications. Briefly, worms were reared at 20°C and moved to room temperature 30 min before imaging. Young adult animals were picked to agar plates with no bacterial lawn (30 worms per plate) and were transferred to second plate lacking bacteria after 5–10 minutes. Worm movement recordings were started 40–45 minutes after the worms were removed from food. 30 second digital videos of individual animals were captured at 5× magnification and 4 Hz frame rate on a Zeiss Discovery Stereomicroscope using Axiovision software. The center of mass was recorded for each animal on each video frame using the object tracking in the Axiovision software. The trajectories were then analyzed using custom software written in Igor Pro 5.0 (Wavemetrics). For all comparisons to untreated wild type controls, statistical significance was determined using the Tukey-Kramer test to control for multiple comparisons. For all pair-wise comparisons of mutant and transgenic rescue strains, statistical significance was determined using a two-tailed Student's t-test.

Fluorescence imaging

All quantitative imaging was done using an Olympus PlanAPO 100× 1.4 NA objective and a CoolSNAP CCD camera (Hamamatsu). Worms were immobilized with 30 mg/ml BDM (Sigma). Image stacks were captured and maximum intensity projections were obtained using Metamorph 7.1 software (Molecular Devices). YFP fluorescence was normalized to the absolute mean fluorescence of 0.5 mm FluoSphere beads (Molecular Probes). For ventral or dorsal cord imaging, young adult worms, in which the ventral or dorsal cords were oriented toward the objective, were imaged in the region just posterior to the vulva. Imaging was done prior to aldicarb treatment and after 60 minutes of 1.5mM aldicarb treatment. Line scans of ventral and dorsal cord fluorescence were analyzed in Igor Pro (WaveMetrics) using custom-written software to identify average peak fluorescence values for all puncta in the imaged region (peak punctal intensity) (Dittman and Kaplan, 2006). For coelomocyte

imaging, the posterior coelomocyte was imaged in larval stage 4 (L4) and early adult worms (Sieburth et al., 2007). For all comparisons to untreated wild type controls, statistical significance was determined using the Tukey-Kramer test to control for multiple comparisons. For all comparisons of control and aldicarb treated animals of the same genotype, statistical significance was determined using a two-tailed Student's t-test.

Electrophysiology

Electrophysiology was done on dissected *C. elegans* as previously described (Richmond and Jorgensen, 1999). Worms were superfused in an extracellular solution containing 127 mM NaCl, 5 mM KCl, 26 mM NaHCO₃, 1.25 mM NaH₂PO₄, 20 mM glucose, 1 mM CaCl₂ and 4 mM MgCl₂, bubbled with 5% CO₂, 95% O₂ at 20°C. Whole cell recordings were carried out at -60 mV using an internal solution containing 105 mM CH₃O₃SCs, 10 mM CsCl, 15 mM CsF, 4 mM MgCl₂, 5mM EGTA, 0.25 mM CaCl₂, 10 mM HEPES and 4 mM Na₂ATP, adjusted to pH 7.2 using CsOH. Under these conditions, we only observed endogenous acetylcholine EPSCs. For endogenous GABA IPSC recordings the holding potential was 0 mV. All recording conditions were as described (McEwen et al., 2006). Stimulus-evoked EPSCs were stimulated by placing a borosilicate pipette (5–10 μm) near the ventral nerve cord (one muscle distance from the recording pipette) and applying a 0.4 ms, 30 μA square pulse using a stimulus current generator (WPI). For aldicarb exposure, a single adult worm was transferred to a plate containing 1mM aldicarb for 60 minutes prior to the dissection, with one exception, *ckr-2* ACh rescue animals were treated for 30 minutes. For all comparisons to untreated wild type controls, statistical significance was determined using the Tukey-Kramer test to control for multiple comparisons. For all comparisons of control and aldicarb treated animals of the same genotype, statistical significance was determined using a two-tailed Student's t-test.

Supplementary Material

Refer to Web version on PubMed Central for supplementary material.

Acknowledgments

We thank the following for strains and reagents: Liliane Schoofs, Tom Janssen, Shawn Xu, and the *C. elegans* Genetics Stock Center. We thank members of the Kaplan lab for critical comments on the manuscript. This work was supported by an NIH research grant to J.K. (DK80215).

References

- Ch'ng Q, Sieburth D, Kaplan JM. Profiling synaptic proteins identifies regulators of insulin secretion and lifespan. *PLoS Genet.* 2008; 4:e1000283. [PubMed: 19043554]
- Chalasan SH, Kato S, Albrecht DR, Nakagawa T, Abbott LF, Bargmann CI. Neuropeptide feedback modifies odor-evoked dynamics in *Caenorhabditis elegans* olfactory neurons. *Nat Neurosci.* 2010; 13:615–621. [PubMed: 20364145]
- Davies AG, Bettinger JC, Thiele TR, Judy ME, McIntire SL. Natural variation in the *npr-1* gene modifies ethanol responses of wild strains of *C. elegans*. *Neuron.* 2004; 42:731–743. [PubMed: 15182714]
- Dittman JS, Kaplan J. Behavioral impact of neurotransmitter-gated GPCRs: Muscarinic and GABAB receptors regulate *C. elegans* locomotion. *Journal of Neuroscience.* 2008; 28:7104–7112. [PubMed: 18614679]
- Dittman JS, Kaplan JM. Factors regulating the abundance and localization of synaptobrevin in the plasma membrane. *Proc Natl Acad Sci U S A.* 2006; 103:11399–11404. [PubMed: 16844789]
- Edwards SL, Charlie NK, Richmond JE, Hegermann J, Eimer S, Miller KG. Impaired dense core vesicle maturation in *Caenorhabditis elegans* mutants lacking Rab2. *J Cell Biol.* 2009; 186:881–895. [PubMed: 19797080]

- Gracheva EO, Burdina AO, Holgado AM, Berthelot-Grosjean M, Ackley BD, Hadwiger G, Nonet ML, Weimer RM, Richmond JE. Tomosyn inhibits synaptic vesicle priming in *Caenorhabditis elegans*. *PLoS Biol.* 2006; 4:e261. [PubMed: 16895441]
- Gracheva EO, Burdina AO, Touroutine D, Berthelot-Grosjean M, Parekh H, Richmond JE. Tomosyn negatively regulates CAPS-dependent peptide release at *Caenorhabditis elegans* synapses. *J Neurosci.* 2007; 27:10176–10184. [PubMed: 17881523]
- Husson SJ, Clynen E, Baggerman G, Janssen T, Schoofs L. Defective processing of neuropeptide precursors in *Caenorhabditis elegans* lacking proprotein convertase 2 (KPC-2/EGL-3): mutant analysis by mass spectrometry. *J Neurochem.* 2006; 98:1999–2012. [PubMed: 16945111]
- Husson SJ, Janssen T, Baggerman G, Bogert B, Kahn-Kirby AH, Ashrafi K, Schoofs L. Impaired processing of FLP and NLP peptides in carboxypeptidase E (EGL-21)-deficient *Caenorhabditis elegans* as analyzed by mass spectrometry. *J Neurochem.* 2007; 102:246–260. [PubMed: 17564681]
- Husson SJ, Schoofs L. Altered neuropeptide profile of *Caenorhabditis elegans* lacking the chaperone protein 7B2 as analyzed by mass spectrometry. *FEBS Lett.* 2007; 581:4288–4292. [PubMed: 17707816]
- Ignell R, Root CM, Birse RT, Wang JW, Nassel DR, Winther AM. Presynaptic peptidergic modulation of olfactory receptor neurons in *Drosophila*. *Proc Natl Acad Sci U S A.* 2009; 106:13070–13075. [PubMed: 19625621]
- Jacob TC, Kaplan JM. The EGL-21 carboxypeptidase E facilitates acetylcholine release at *Caenorhabditis elegans* neuromuscular junctions. *J Neurosci.* 2003; 23:2122–2130. [PubMed: 12657671]
- Janssen T, Meelkop E, Lindemans M, Verstraelen K, Husson SJ, Temmerman L, Nachman RJ, Schoofs L. Discovery of a cholecystokinin-gastrin-like signaling system in nematodes. *Endocrinology.* 2008; 149:2826–2839. [PubMed: 18339709]
- Jockusch WJ, Speidel D, Sigler A, Sorensen JB, Varoqueaux F, Rhee JS, Brose N. CAPS-1 and CAPS-2 are essential synaptic vesicle priming proteins. *Cell.* 2007; 131:796–808. [PubMed: 18022372]
- Kang L, Gao J, Schafer WR, Xie Z, Xu XZ. *C. elegans* TRP Family Protein TRP-4 Is a Pore-Forming Subunit of a Native Mechanotransduction Channel. *Neuron.* 2010; 67:381–391. [PubMed: 20696377]
- Kass J, Jacob TC, Kim P, Kaplan JM. The EGL-3 proprotein convertase regulates mechanosensory responses of *Caenorhabditis elegans*. *J Neurosci.* 2001; 21:9265–9272. [PubMed: 11717360]
- Kawaguchi Y, Kondo S. Parvalbumin, somatostatin and cholecystokinin as chemical markers for specific GABAergic interneuron types in the rat frontal cortex. *J Neurocytol.* 2002; 31:277–287. [PubMed: 12815247]
- Lear BC, Merrill CE, Lin JM, Schroeder A, Zhang L, Allada R. A G protein-coupled receptor, groom-of-PDF, is required for PDF neuron action in circadian behavior. *Neuron.* 2005; 48:221–227. [PubMed: 16242403]
- Li, C.; Kim, K. Neuropeptides. *WormBook*; 2008. p. 1-36.
- Li W, Feng Z, Sternberg PW, Xu XZ. A *C. elegans* stretch receptor neuron revealed by a mechanosensitive TRP channel homologue. *Nature.* 2006; 440:684–687. [PubMed: 16572173]
- McEwen JM, Madison JM, Dybbs M, Kaplan JM. Antagonistic Regulation of Synaptic Vesicle Priming by Tomosyn and UNC-13. *Neuron.* 2006; 51:303–315. [PubMed: 16880125]
- McVeigh P, Leech S, Marks NJ, Geary TG, Maule AG. Gene expression and pharmacology of nematode NLP-12 neuropeptides. *Int J Parasitol.* 2006; 36:633–640. [PubMed: 16600246]
- Mertens I, Vandingenen A, Johnson EC, Shafer OT, Li W, Trigg JS, De Loof A, Schoofs L, Taghert PH. PDF receptor signaling in *Drosophila* contributes to both circadian and geotactic behaviors. *Neuron.* 2005; 48:213–219. [PubMed: 16242402]
- Miller KG, Alfonso A, Nguyen M, Crowell JA, Johnson CD, Rand JB. A genetic selection for *Caenorhabditis elegans* synaptic transmission mutants. *Proc Natl Acad Sci U S A.* 1996; 93:12593–12598. [PubMed: 8901627]

- Moore MS, DeZazzo J, Luk AY, Tully T, Singh CM, Heberlein U. Ethanol intoxication in *Drosophila*: Genetic and pharmacological evidence for regulation by the cAMP signaling pathway. *Cell*. 1998; 93:997–1007. [PubMed: 9635429]
- Mullen GP, Mathews EA, Saxena P, Fields SD, McManus JR, Moulder G, Barstead RJ, Quick MW, Rand JB. The *Caenorhabditis elegans* snf-11 gene encodes a sodium-dependent GABA transporter required for clearance of synaptic GABA. *Mol Biol Cell*. 2006; 17:3021–3030. [PubMed: 16641366]
- Nonet M, Saifee O, Zhao H, Rand J, Wei L. Synaptic transmission deficits in *Caenorhabditis elegans* synaptobrevin mutants. *J Neurosci*. 1998; 18:70–80. [PubMed: 9412487]
- Nurrish S, Segalat L, Kaplan J. Serotonin inhibition of synaptic transmission: GOA-1 decreases the abundance of UNC-13 at release sites. *Neuron*. 1999; 24:231–242. [PubMed: 10677040]
- Renn SC, Park JH, Rosbash M, Hall JC, Taghert PH. A pdf neuropeptide gene mutation and ablation of PDF neurons each cause severe abnormalities of behavioral circadian rhythms in *Drosophila*. *Cell*. 1999; 99:791–802. [PubMed: 10619432]
- Saifee O, Wei L, Nonet ML. The *Caenorhabditis elegans* unc-64 Locus Encodes a Syntaxin That Interacts Genetically with Synaptobrevin. *Mol Biol Cell*. 1998; 9:1235–1252. [PubMed: 9614171]
- Sieburth D, Ch'ng Q, Dybbs M, Tavazoie M, Kennedy S, Wang D, Dupuy D, Rual JF, Hill DE, Vidal M, et al. Systematic analysis of genes required for synapse structure and function. *Nature*. 2005; 436:510–517. [PubMed: 16049479]
- Sieburth D, Madison JM, Kaplan JM. PKC-1 regulates secretion of neuropeptides. *Nat Neurosci*. 2007; 10:49–57. [PubMed: 17128266]
- Speese S, Petrie M, Schuske K, Ailion M, Ann K, Iwasaki K, Jorgensen EM, Martin TF. UNC-31 (CAPS) is required for dense-core vesicle but not synaptic vesicle exocytosis in *Caenorhabditis elegans*. *J Neurosci*. 2007; 27:6150–6162. [PubMed: 17553987]
- Sumakovic M, Hegermann J, Luo L, Husson SJ, Schwarze K, Olendrowitz C, Schoofs L, Richmond J, Eimer S. UNC-108/RAB-2 and its effector RIC-19 are involved in dense core vesicle maturation in *Caenorhabditis elegans*. *J Cell Biol*. 2009; 186:897–914. [PubMed: 19797081]
- Vashlishan AB, Madison JM, Dybbs M, Bai J, Sieburth D, Ch'ng Q, Tavazoie M, Kaplan JM. An RNAi screen identifies genes that regulate GABA synapses. *Neuron*. 2008; 58:346–361. [PubMed: 18466746]
- White JG, Southgate E, Thomson JN, Brenner S. The structure of the nervous system of *Caenorhabditis elegans*. *Philos Trans R Soc Lond*. 1986; 314:1–340.
- Wicks SR, Rankin CH. Integration of mechanosensory stimuli in *C. elegans*. *J Neurosci*. 1995; 15:2434–2444. [PubMed: 7891178]
- Wicks SR, Roehrig CJ, Rankin CH. A dynamic network simulation of the nematode tap withdrawal circuit: predictions concerning synaptic function using behavioral criteria. *J Neurosci*. 1996; 16:4017–4031. [PubMed: 8656295]

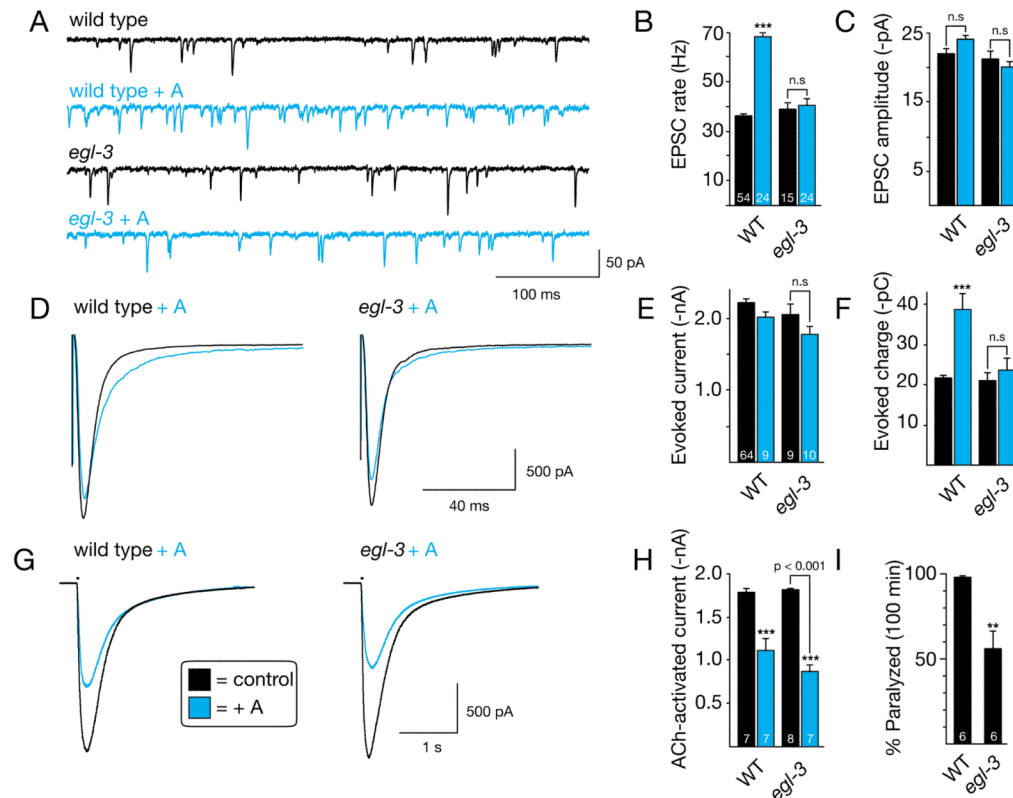


Figure 1. Electrophysiological characterization of *egl-3* mutants

Endogenous EPSCs (A–C), stimulus-evoked EPSCs (D–F), and ACh-evoked currents (G–H) were recorded from body wall muscle of adult worms of the indicated genotypes, with (blue) and without (black) a 60 minute aldicarb treatment. Representative traces of endogenous EPSCs (A), averaged traces of stimulus-evoked responses (D) and ACh-evoked currents (G), and summary data for all three are shown (B, C, E, F, H). (I) Aldicarb-induced paralysis is compared for the indicated genotypes. The number of animals analyzed (B, E, H) or the number of replicate experiments (I) is indicated for each genotype. Values that are significantly different from untreated wild type controls are indicated (***, $p < 0.001$; **, $p < 0.01$). Error bars indicate SEM. A common set of wild recordings (+ and – aldicarb) were utilized in Figs. 1, 2, 3, and 5. All comparisons to this control data set were corrected for multiple comparisons using the Tukey-Kramer test. All electrophysiological data are shown in Table S1.

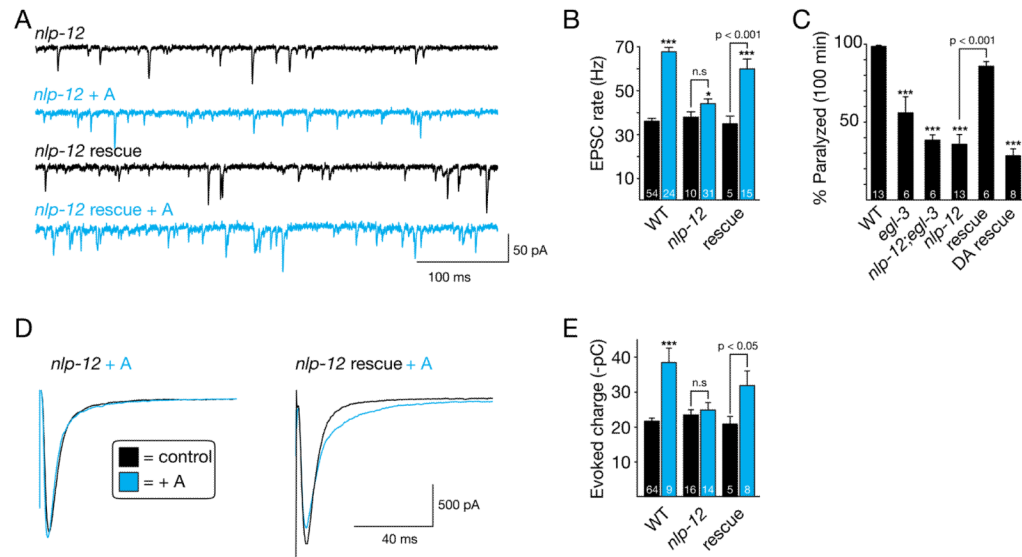


Figure 2. The neuropeptide NLP-12 is required for aldicarb induced potentiation of cholinergic transmission

Endogenous EPSCs (A–B) and stimulus-evoked EPSCs (D–E) were recorded from body wall muscle of adult worms of the indicated genotypes, with (blue) and without (black) a 60 minute aldicarb treatment. Representative traces of endogenous EPSCs (A), averaged stimulus-evoked responses (D), and summary data (B, E) are shown. (C) Aldicarb-induced paralysis is compared for the indicated genotypes. Rescue refers to *nlp-12* mutants carrying a transgene containing a 2.1kb genomic *nlp-12* clone in which YFP was fused at the NLP-12 carboxy terminus. DA Rescue refers to *nlp-12* mutants carrying a transgene expressing NLP-12 in DA motor neurons (using the *unc-129* promoter). The number of animals analyzed (B, E) or the number of replicate experiments (C) is indicated for each genotype. Values that are significantly different from untreated wild type controls are indicated (***, $p < 0.001$). Error bars indicate SEM. A common set of wild recordings (+ and – aldicarb) were utilized in Figs. 1, 2, 3, and 5. All comparisons to this control data set were corrected for multiple comparisons using the Tukey-Kramer test. All electrophysiological data are shown in Table S2.

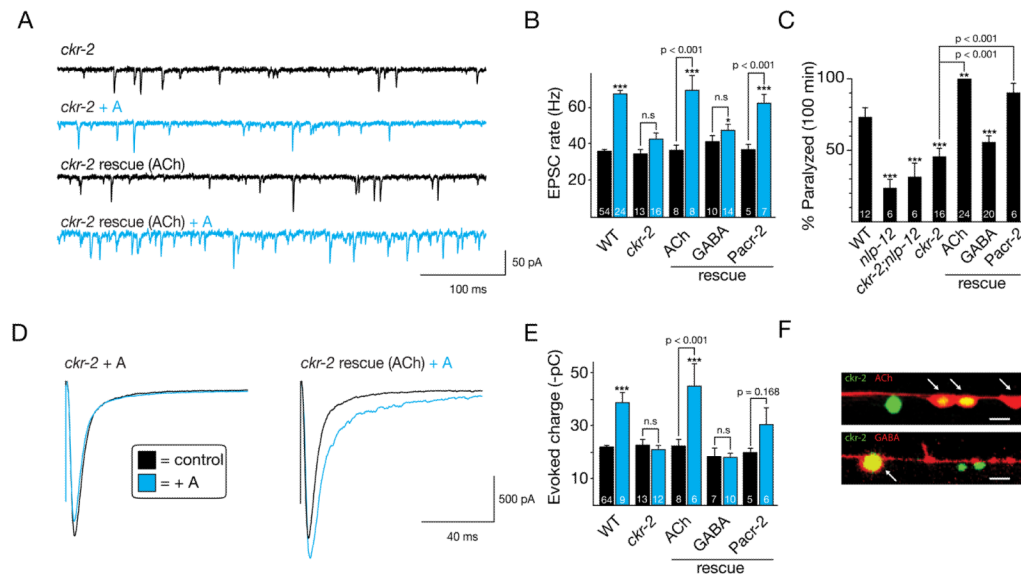


Figure 3. The NLP-12 receptor CKR-2 is also required for suppression of aldicarb induced potentiation

Endogenous EPSCs (A–B) and stimulus-evoked EPSCs (D–E) were recorded from body wall muscle of adult worms of the indicated genotypes, with (blue) and without (black) aldicarb pre-treatment (30 minutes for ACh rescue, 60 minutes for all others). Representative traces of endogenous EPSCs (A), averaged stimulus-evoked responses (D), and summary data (B, E) are shown. *ckr-2* mutants containing transgenes driving CKR-2 expression in all cholinergic neurons (using the *unc-17* promoter) [rescue (ACh)], in GABA neurons (using the *unc-25* promoter) [rescue (GABA)], and in cholinergic motor neurons (using the *acr-2* promoter) [rescue Pacr-2] are indicated. (C) Aldicarb-induced paralysis is compared for the indicated genotypes. The number of animals analyzed (B, E) or the number of replicate experiments (C) is indicated for each genotype. (F) Pckr-2::NLS::GFP expresses in both cholinergic neurons (*Punc-17*::mCherry), in GABA neurons (*Punc-25*::mCherry). Arrows indicated cells bodies. Values that are significantly different from untreated wild type controls are indicated (***, $p < 0.001$; *, $p < 0.05$). Error bars indicate SEM. A common set of wild recordings (+ and – aldicarb) were utilized in Figs. 1, 2, 3, and 5. All comparisons to this control data set were corrected for multiple comparisons using the Tukey-Kramer test. All electrophysiological data are shown in Table S3.

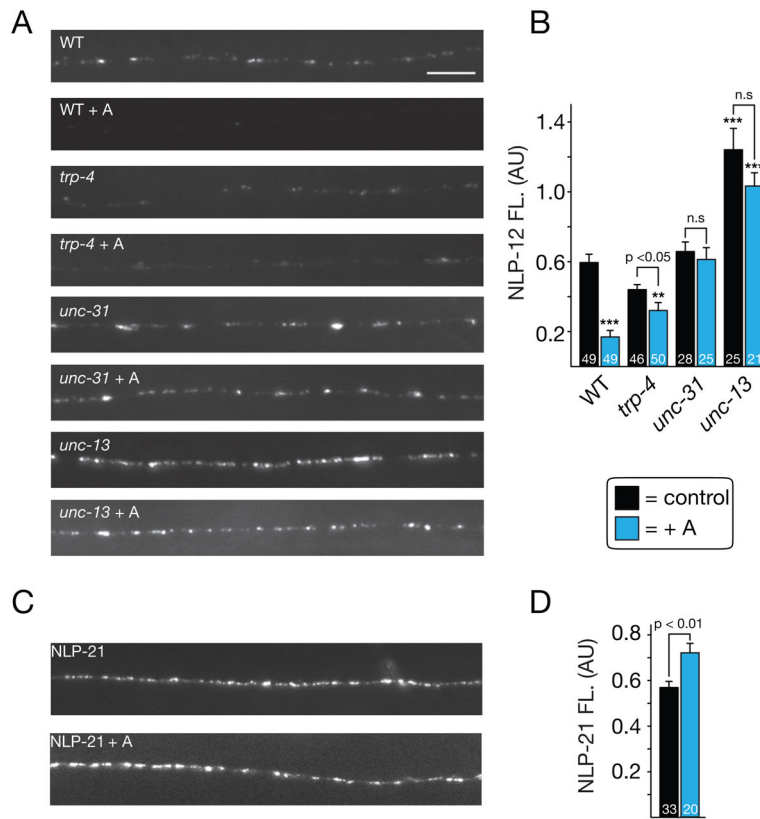


Figure 4. Aldicarb stimulates NLP-12 secretion from DVA neurons

Representative images (A) and summary data (B) for NLP-12::YFP fluorescence in the DVA ventral cord axon are shown for the indicated genotypes, with and without aldicarb treatment. (C–D) Representative images (C) and summary data (D) for NLP-21::YFP fluorescence in the dorsal cord axons of wild type DA motor neurons, with and without aldicarb treatment are shown. The number of animals analyzed is indicated for each genotype. The number of replicate experiments were: 5 WT, 5 *trp-4*, 4 *unc-31*, 4 *unc-13*, 9 NLP-21, and 3 NLP-21+A. Values that are significantly different from untreated wild type controls are indicated (***, $p < 0.001$; **, $p < 0.01$). Error bars indicate SEM.

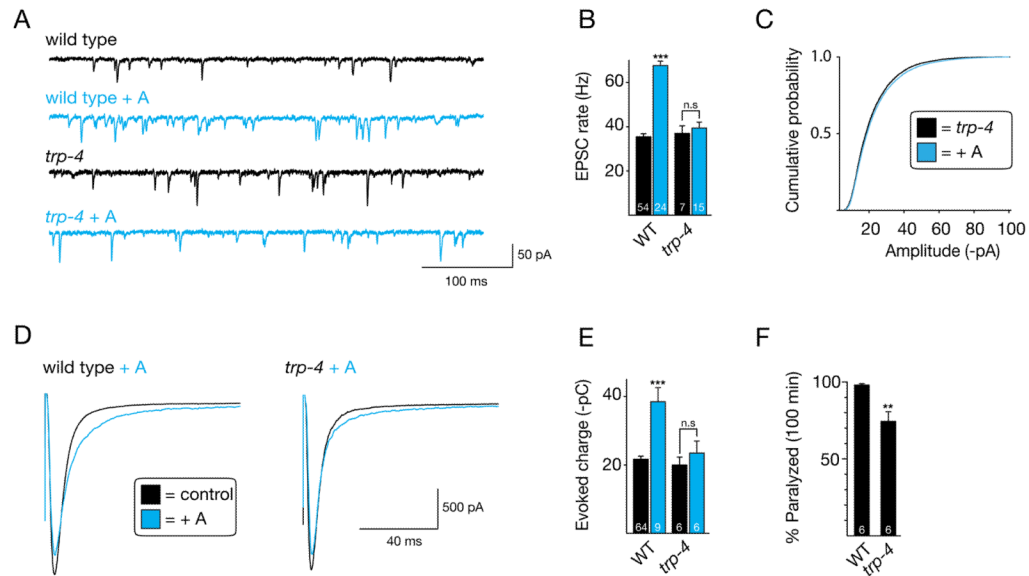


Figure 5. The mechanosensory channel TRP-4 is required for aldicarb induced potentiation of cholinergic transmission

Endogenous EPSCs (A–C) and stimulus-evoked EPSCs (D–E) were recorded from body wall muscle of adult worms of the indicated genotypes, with (blue) and without (black) a 60 minute aldicarb treatment. Representative traces of endogenous EPSCs (A), averaged stimulus-evoked responses (D), and summary data (B, C, E) are shown. (C) Cumulative probability distributions are shown for *trp-4* mutant endogenous EPSC amplitudes, with and without aldicarb treatment. No significant differences were observed. (F) Aldicarb-induced paralysis is compared for the indicated genotypes. The number of animals analyzed (B, E) or the number of replicate experiments (F) is indicated for each genotype. Values that are significantly different from untreated wild type controls are indicated (***, $p < 0.001$; **, $p < 0.01$). Error bars indicate SEM. A common set of wild recordings (+ and – aldicarb) were utilized in Figs. 1, 2, 3, and 5. All comparisons to this control data set were corrected for multiple comparisons using the Tukey-Kramer test. All electrophysiological data are shown in Table S4.

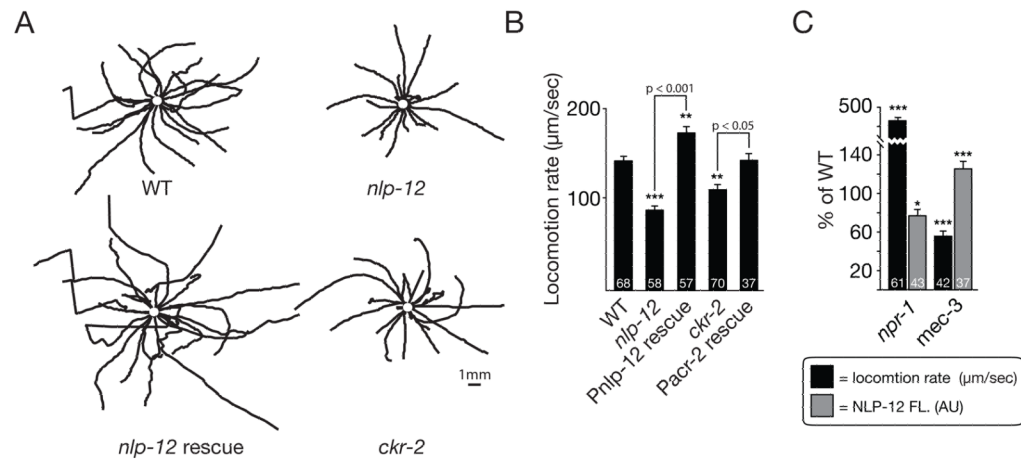


Figure 6. NLP-12 regulates locomotion behavior

(A) Representative 30 second locomotion trajectories are shown (n= 20 animals for each genotype). The starting points for each trajectory were aligned for clarity. (B) Locomotion rates are compared for the indicated genotypes. *Pnlp-12* rescue refers to *nlp-12* mutants carrying a transgene containing a 2.1kb genomic *nlp-12* clone. *Pacr-2* rescue refers to *ckr-2* mutants carrying a transgene driving CKR-2 expression in cholinergic motor neurons (using the *acr-2* promoter). The number of replicate experiments were: 6 WT, 3 *nlp-12*, 3 *nlp-12* rescue, 6 *ckr-2*, and 3 *ckr-2* rescue. (C) Locomotion rates and NLP-12 puncta fluorescence intensities (both normalized to wild type) are shown for *npr-1* and *mec-3* mutants. The number of animals analyzed is indicated for each genotype. The number of replicate experiments were: NLP-12 fluorescence in *npr-1* (6 WT, 6 *npr-1*); NLP-12 fluorescence in *mec-3* (4 WT and 4 *mec-3*); *npr-1* locomotion (3 WT and 3 *npr-1*); *mec-3* locomotion (6 WT and 3 *mec-3*). Values that are significantly different from wild type are indicated (***, $p < 0.001$; **, $p < 0.01$; *, $p < 0.05$). Error bars indicate SEM.